Euro. Jnl of Applied Mathematics (2013), *vol.* 24, *pp.* 343–370. © Cambridge University Press 2012
doi:10.1017/S0956792512000435

Refinements to the study of electrostatic deflections: theory and experiment

N. D. BRUBAKER[1], J. I. SIDDIQUE[2], E. SABO[1], R. DEATON[1] and J. A. PELESKO[1]

[1]*Department of Mathematical Sciences, University of Delaware, Newark, DE 19716, USA*
email: brubaker@math.udel.edu, esabo@udel.edu, rdeaton@udel.edu, pelesko@math.udel.edu
[2]*Department of Mathematics, Pennsylvania State University, York Campus, 1031 Edgecomb Avenue, York, PA 17403, USA*
email: ji15@psu.edu

(*Received 6 March 2012; revised 9 November 2012; accepted 12 November 2012; first published online 14 December 2012*)

To study electrostatic actuation, researchers commonly use a setup proposed by G. I. Taylor in [Proc. R. Soc. Lond. Ser. A, 306 (1968), pp. 423–434]. It consists of soap film held at a distance h above a rigid plate so that when a voltage difference is applied between the two components, the top film deflects towards the bottom plate. The most striking feature of this system is when the voltage difference exceeds a critical value V^*, the electrostatic forces dominate the surface forces and the soap film gets 'pulled-into' or collapses onto the bottom plate. This so-called 'pull-in' instability is a ubiquitous feature of electrostatic actuation and as a result, has been the subject of many studies. Recently, Siddique *et al.* [J. Electrostatics, 69 (2011), pp. 1–6] measured the value of V^* as a function of the separation distance and found that the standard prediction breaks down as h increases. Here, we continue the work done in [N. D. Brubaker and J. A. Pelesko, European J. Appl. Math., 22 (2011), pp. 455–470] by investigating the cause of this discrepancy. Specifically, we model the effect of gravity on the generalized version of Taylor's model and study whether it provides the proper correction to the predicted value of V^*. In doing so, we derive two nonlinear eigenvalue value problems and investigate their solutions sets.

Key words: Electrostatic actuation; Pull-in voltage; Nonlinear elliptic PDE; Prescribed mean curvature; Nonlinear eigenvalue

1 Introduction

The modern study of electrostatic deflections was started in the late 1960s when the famous fluid mechanician G. I. Taylor analysed the coalescence of soap bubbles held at different electric potentials [23]. To do so he placed soap films on the ends of two electrically isolated, conducting tubes and then applied a voltage difference between them. This produced an attractive force between the two films, causing them to deflect towards each other. Taylor then studied the shape of these deflections as a function of the potential difference and the gap between the tubes. The most impactful and surprising observation of this work was that when the voltage difference is increased beyond some critical value V^*, the two films suddenly snap together or 'pull-in' – accordingly named the 'pull-in' instability.

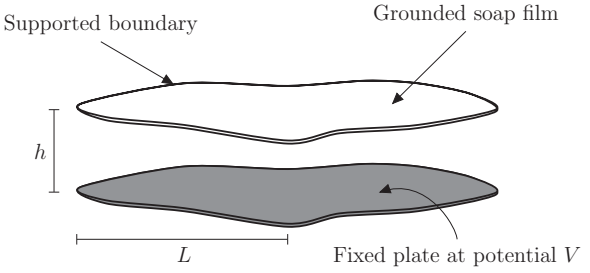

FIGURE 1. Canonical setup.

While Taylor's research was motivated by the interaction of water droplets in an electrified cloud, his work has found applications in the field of micro-electromechanical systems (MEMS), where the soap films are replaced by thin silicon wafers. However, in this context the pull-in instability severely limits the design space of MEMS devices and therefore is one of the keys to fully understanding MEMS behaviour [18].

The well-known, general version of Taylor's setup that we will concern ourselves with is the one shown in Figure 1. In dimensionless form, this situation can be modelled by the following boundary value problem [4]:

$$\operatorname{div} \frac{\nabla u}{\sqrt{1+\varepsilon^2|\nabla u|^2}} = \frac{\lambda}{(1+u)^2} \quad \text{in} \quad \Omega; \qquad u = 0 \quad \text{in} \quad \partial\Omega. \tag{1.1 a, b}$$

Here the function $u : \bar{\Omega} \to (-1, 0]$ describes the shape of the deflected membrane and Ω is a open set in $\mathbb{R}^2$ with a piecewise smooth boundary $\partial\Omega$. The non-negative dimensionless parameters ε and λ are defined as

$$\varepsilon = \frac{h}{L}, \qquad \lambda = \frac{\varepsilon_0 V^2 L^2}{2\gamma h^3}, \tag{1.2}$$

where ε_0 is the permittivity of free space, V is the potential difference between the membrane and the plate, L is the characteristic size of the membrane, h is the vertical distance between the boundary of the plate and the boundary of the membrane and γ is the surface tension of the membrane. To derive equation (1.1 *a*), we note that the the aspect ratio ε must be small. When $\varepsilon = 0$, the model reduces the standard 'MEMS equation' and has studied by numerous authors [1, 10, 17, 19, 20, 23]. The case where $\varepsilon \neq 0$ has recently been studied too [3–5]. The key feature of model (1.1) is that it captures the pull-in instability via the following fact: for all $\varepsilon \geqslant 0$, there exists a λ^* such that no solutions of boundary value problem (1.1) exist for any $\lambda > \lambda^*$ (see [18, §7.5.1] and [4]). Since $\lambda \propto V^2$, this statement is equivalent to increasing the applied voltage beyond the critical threshold V^*. As a result the value of λ^* provides a prediction for the pull-in voltage

$$V^* = \frac{\sqrt{2\gamma\lambda^*}}{\sqrt{\varepsilon_0} L} h^{3/2}, \tag{1.3}$$

https://doi.org/10.1017/S0956792512000435 Published online by Cambridge University Press

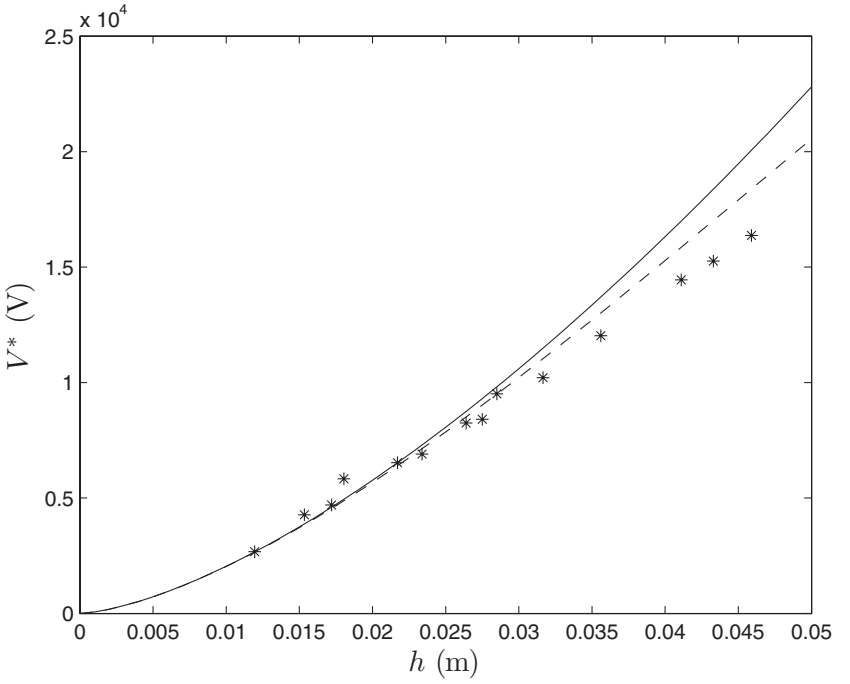

FIGURE 2. Leading order approximation (line) and the two-term expansion (dashed line) of the pull-in voltage V^* (from (1.5)) versus the plate separation h with the experimental data (asterisk) from [22].

where $\lambda^* = \lambda^*(\Omega, \varepsilon)$ and $V^* = V^*(\Omega, \varepsilon)$. For Ω equal to the unit disk $\mathscr{D}_1$ the physical accuracy of this prediction can be tested by using the two-term asymptotic expansion

$$\lambda^* = \lambda_0^* + \varepsilon^2 \lambda_s + \mathcal{O}(\varepsilon^2), \quad \varepsilon \ll 1, \tag{1.4}$$

from [4] in (1.3). Here $\lambda_0^* = \lambda^*(\mathscr{D}_1, 0)$ and λ_s is the correction due to inclusion of the full surface effects. They are approximately 0.7892 and -0.1360, respectively. This yields

$$V^* \sim \sqrt{\frac{2\gamma\lambda_0^*}{\varepsilon_0 L^2}} h^{3/2} + \frac{\lambda_s \sqrt{\gamma}}{\sqrt{2\varepsilon_0 \lambda_0} L^3} h^{7/2}, \tag{1.5}$$

on $\Omega = \mathscr{D}_1$, for $h \ll 1$ [4]. In comparing this approximation (1.5) with data collected in [22] it is found that (1.5) does indeed provide an accurate prediction of the pull-in voltage [4] for very small plate separation h (see Figure 2); however, as h is increased the accuracy of this prediction breaks down, suggesting that there are other important effects in this regime. Two likely sources are the gravitational and fringing fields. In this paper, we look at the former. Specifically, we investigate how gravity affects the generalized version of Taylor's experiment (Figure 1) and see if it causes the aforementioned discrepancy. To do this, we first derive a general model that includes surface, electrostatic and gravitational forces. From various assumptions, we then reduce this general model to two simplified models and then investigate their effect the theoretical value of V^*. Finally, we compare

https://doi.org/10.1017/S0956792512000435 Published online by Cambridge University Press

these predictions to experimental data. As a result, we find that the gravity plays a negligible role, suggesting that a correction needs to be made in the electric field.

The remainder of the paper is organized as follows. We begin the next section by deriving a general model of the system shown in Figure 1 that includes the effect of gravity. We then use the following three approximations to reduce the general model to model (1.1) with $\varepsilon = 0$: one, the fringing fields are negligible; two, the effect of gravity is small; three, the membrane film undergoes small deflections so the norm of the gradient is small. While the first assumption is used throughout, in the next two sections we investigate the effects of removing assumptions two and three. Specifically, in Section 3 we investigate the effects of removing assumption two, and in Section 4 we investigate the effects of removing both assumptions two and three. In each the existence of λ^* is shown, and the behaviour of λ^* is studied using perturbation methods. Then in Section 5 we use the results of Sections 3 and 4 to formulate predicted pull-in voltages of the models, which we compare to experimental data. Lastly, we conclude by commenting on the effects of gravity.

2 Model

In this section, we present the governing equations for the dimensionless shape u of an electrostatically actuated soap film. The system we study is the generalized version of Taylor's setup shown in Figure 1. Specifically, a soap film $\tilde{\Sigma}$ with fixed boundary $\partial\tilde{\Omega}$ is suspended at distance h above a rigid plate. A voltage difference is then applied between the components (we take the plate to have potential V and soap film to be grounded), creating an electrostatic force that deflects the soap film. To the model shape of the deflection we first assume that the soap film $\tilde{\Sigma}$ can be represented by the graph $\tilde{z} = \tilde{u}(\tilde{x}, \tilde{y})$ over the domain $\tilde{\Omega}$ (which, without loss of generality, contains the origin). Then in denoting the electrostatic potential by $\tilde{\psi}(\tilde{x}, \tilde{y}, \tilde{z})$, we find that the total energy $\tilde{\mathscr{E}}$ of the system is given by

$$\tilde{E} = \gamma \iint_{\tilde{\Sigma}} \mathrm{d}\tilde{\sigma} + \rho g \ell \iint_{\tilde{\Sigma}} \tilde{u}\, \mathrm{d}\tilde{\sigma} + \frac{\varepsilon_0}{2} \iint_{\tilde{\Omega}} \int_{-h}^{\tilde{u}} |\tilde{\nabla}\tilde{\psi}|^2 \, \mathrm{d}\tilde{z}\, \mathrm{d}\tilde{x}\, \mathrm{d}\tilde{y}, \tag{2.1}$$

where the terms are due to the surface energy of the film [7], the gravitational potential energy of the film and the potential energy of the electric field [11], respectively. The constants γ, ρ and ℓ are the surface tension, density and thickness of the film, respectively. Also, g is the gravitational acceleration of Earth and ε_0 is the permittivity of free space. Note that g can be taken to be positive or negative, corresponding to gravity pointing down or up in the vertical direction. We next introduce the dimensionless variables

$$x = \tilde{x}/L, \quad y = \tilde{y}/L, \quad z = \tilde{z}/h, \quad u = \tilde{u}/h, \quad \psi = \tilde{\psi}/V, \tag{2.2}$$

where L is the maximum radial distance of $\tilde{\Omega}$, i.e. $L = \max\{|\tilde{x}| : \tilde{x} \in \partial\tilde{\Omega}\}$. Substituting these into energy (2.1) yields the dimensionless energy

$$E = \frac{1}{\varepsilon^2} \iint_{\Sigma} \mathrm{d}\sigma + \beta \iint_{\Sigma} u\, \mathrm{d}\sigma + \lambda \iint_{\Omega} \int_{-1}^{u} \left(\varepsilon^2 |\nabla_2 \psi|^2 + {\psi_z}^2\right) \mathrm{d}z\, \mathrm{d}x\, \mathrm{d}y, \tag{2.3}$$

https://doi.org/10.1017/S0956792512000435 Published online by Cambridge University Press

where the notation $\nabla_2\psi$ indicates differentiation is only with respect to x and y. The non-negative dimensionless parameters λ and ε are the same as in problem (1.1). The dimensionless parameter β is the Bond number $\rho g \ell L^2/(\gamma h)$ and measures the relative importance of gravity versus surface tension.

Finally by minimizing (2.3) using the first variational derivative, we obtain the following coupled system of partial differential equations for the shape of the deflected membrane u and the electrostatic potential ψ:

$$\varepsilon^2 \Delta_2 \psi + \frac{\partial^2 \psi}{\partial z^2} = 0, \tag{2.4a}$$

in the region between the soap film and the plate, and

$$(1 + \varepsilon^2 \beta u)\,\mathrm{div}\,\frac{\nabla u}{\sqrt{1+\varepsilon^2|\nabla u|^2}} = \lambda\left(\varepsilon^2\,|\nabla_2\psi|^2 + {\psi_z}^2\right) + \frac{\beta}{\sqrt{1+\varepsilon^2|\nabla u|^2}}, \tag{2.4b}$$

in $\Omega \times \{z = u(x,y)\}$. Here, Ω is a bounded domain in $\mathbb{R}^2$ with boundary $\partial\Omega$ whose maximum radial distance is less than or equal to 1 (due to (2.2)). To complete the general model, we require that the boundary of the soap film stay fixed

$$u = 0 \quad \text{on} \quad \partial\Omega. \tag{2.4c}$$

Also since the soap film is grounded and the plate is held at voltage V, we have

$$\psi = 0 \quad \text{on} \quad \Omega \times \{z = u\}, \qquad \psi = 1 \quad \text{on} \quad \Omega \times \{z = -1\}. \tag{2.4d}$$

Remark 2.1 For system (2.4) – and all the resulting boundary value problems derived from it – we look for solutions such that $u > -1$ in Ω so, in physical terms, the membrane does not hit the bottom plate.

This general model of electrostatic actuation is a nonlinear system of partial differential equations that is coupled in two ways: one, the first source term on the right-hand side of (2.4b) captures the force on the film due to the electric field; two, since the top membrane is grounded, the potential depends on the deflection of the elastic plate. Because of the complexity of (2.4), researchers have used various assumptions to simplify the model.

The first is that the fringing field present in the electric field has negligible effect on the film. As a result the order $\mathcal{O}(\varepsilon^2)$ terms due to the potential ψ are dropped and equation (2.4) can be solved. This then reduces system (2.4) to

$$\begin{aligned} &(1 + \beta\varepsilon^2 u)\,\mathrm{div}\,\frac{\nabla u}{\sqrt{1+\varepsilon^2|\nabla u|^2}} = \frac{\lambda}{(1+u)^2} + \frac{\beta}{\sqrt{1+\varepsilon^2|\nabla u|^2}} && \text{in } \Omega, \\ &u = 0 && \text{on } \partial\Omega. \end{aligned} \tag{2.5}$$

The second is that the gravitational effects on the film are minor. Namely β is taken to be zero, and boundary value problem (2.5) becomes (1.1).

https://doi.org/10.1017/S0956792512000435 Published online by Cambridge University Press

The last, due to the small aspect ratio, is that the top plate undergoes only small deflections so that the $\varepsilon^2|\nabla u|^2$ terms are very small. In omitting these derivatives, the left-hand side of equation (1.1 *a*) becomes the Laplacian and boundary value problem (1.1) reduces to the standard 'MEMS model'.

In the next two sections, we investigate the effects of non-negligible gravity with and without the small deflection approximation.

3 The effect of gravity on the canonical model

In this section, we study the effects of non-negligible gravity on the MEMS equation. Specifically, we take ε to zero so that governing boundary value problem (2.5) becomes a semi-linear elliptic partial differential equation with homogeneous Dirichlet boundary conditions

$$\Delta u = \frac{\lambda}{(1+u)^2} + \beta \quad \text{in} \quad \Omega, \qquad u = 0 \quad \text{in} \quad \partial\Omega, \tag{3.1}$$

where physically $\beta \ll 1$. While for our defined β this system models the effects of gravity, more generally (3.1) models the deflection of an MEMS capacitor due to the presence of an external pressure (see, e.g. [1, 2, 23]). For these systems, Beckham [2] examined the existence and non-existence of solutions depending on β and λ and specifically, showed the existence of a λ^*.

Theorem 3.1 (Beckham [[2], §3.3.1]) *Let Ω be a bounded domain in $\mathbb{R}^2$ with boundary $\partial\Omega$. For every fixed value of β, there exists a λ^* such that no solutions of boundary value problem* (3.1) *exist for $\lambda > \lambda^*$.*

In addition, we can prove a parallel result for β. That is, for all $\lambda > 0$ there exists a β^* such that no classical solutions of the boundary value problem (3.1) exist for $\beta \geqslant \beta^*$. We should remark that this result has been observed for specific domains (cf. [1, 2, 23]); however, no rigorous proof exists – specific domain or otherwise. To this end, we first prove the following lemma.

Lemma 3.2 *Let $\beta \geqslant 0$, Ω be a bounded domain with boundary $\partial\Omega$ and u in $C^2(\Omega) \cap C(\bar{\Omega})$ solve boundary value problem* (3.1). *Furthermore, assume that v in $C^2(\Omega) \cap C(\bar{\Omega})$ is the unique solution to*

$$\Delta v = \beta \quad \text{in} \quad \Omega, \qquad v = 0 \quad \text{in} \quad \partial\Omega. \tag{3.2}$$

Then, for all x in $\bar{\Omega}$, $u(x) \leqslant v(x)$.

Proof Since λ and β are greater than or equal to zero, $\lambda(1+u)^{-2} + \beta \geqslant \beta$, and, by comparison theorem for sub-harmonic functions [21], $u \leqslant v$ in $\bar{\Omega}$. □

From this, we prove the following.

https://doi.org/10.1017/S0956792512000435 Published online by Cambridge University Press

Theorem 3.3 *Let Ω be a bounded domain with boundary $\partial\Omega$. Define*

$$\beta^* := \min\left\{\beta \geqslant 0 : \min_{x\in\Omega} v(x;\beta) \leqslant -1\right\}, \tag{3.3}$$

where $v(\cdot;\beta)$ in $C^2(\Omega)\cap C(\bar{\Omega})$ is the unique solution of (3.2). *If $\beta \geqslant \beta^*$, then boundary value problem* (3.1) *has no solutions in $C^2(\Omega)\cap C(\bar{\Omega})$.*

Proof Assume to the contrary that there exists a solution u in $C^2(\Omega)\cap C(\bar{\Omega})$ to boundary value problem (3.1). Then, by Lemma 3.2, the solution $u \leqslant v$ for all x in Ω, which implies $\min_{x\in\Omega} u(x) \leqslant \min_{x\in\Omega} v(x;\beta) \leqslant \min_{x\in\Omega} v(x;\beta^*) \leqslant -1$; however, this is a contradiction, and we have our result. □

Corollary 3.4 *For all $\lambda > 0$, there exists a β^* such that no solutions in $C^2(\Omega)\cap C(\bar{\Omega})$ of boundary value problem* (3.1) *exist for $\beta \geqslant \beta^*$.*

Remark 3.5 We also note from definition (3.3) that the value β^* depends on the shape of the domain Ω; in particular, we have $\beta^* = \beta^*(\Omega)$.

Now that we have some general results for model (3.1), let us look at the case where Ω is the unit disk $\mathscr{D}_1$. From Theorem 3.3 we have that $v(r;\beta) = \beta(r^2-1)/4$. Hence, $\beta^* = 4$, meaning no solutions of (3.1) on $\mathscr{D}_1$ exist for $\beta \geqslant 4$. Also by Theorem 1 of [8], if $\beta \geqslant 0$, then solutions must be radially symmetric. That is, $u(x) = u(r)$, where $r = |x|$, and boundary value problem (3.1) becomes

$$u'' + \frac{1}{r}u' = \frac{\lambda}{(1+u)^2} + \beta, \quad 0 < r < 1; \qquad u'(0) = u(1) = 0. \tag{3.4}$$

If $\beta < 0$, this is not necessarily true. However, for simplicity we only look for radial solutions of (3.1) in this situation as well. To compute the bifurcation diagram for fixed β in $(-\infty, 4)$, we use a shooting method by imposing the initial conditions

$$u'(0) = 0, \qquad u(0) = \alpha > -1, \tag{3.5}$$

and finding λ such that $u(1) = 0$. In doing this, we obtain bifurcation diagrams for various β, which are given in Figure 3. For a more rigorous analysis of the solution set, see [2].

3.1 Asymptotic analysis

Next, we construct two parts of the solution curve of (3.4) for $\beta \ll 1$ via perturbation methods. The first is the infinite fold structure for $u(0)$ near -1 and the second is the location of the fold point corresponding to λ^*.

3.1.1 *The infinite fold structure*

To analyse the infinite fold structure of (3.4) we implement the method of Lindsay and Ward [13] by setting $u(0) = -1 + \delta$ and looking at the regime where $0 < \delta \ll 1$ and

https://doi.org/10.1017/S0956792512000435 Published online by Cambridge University Press

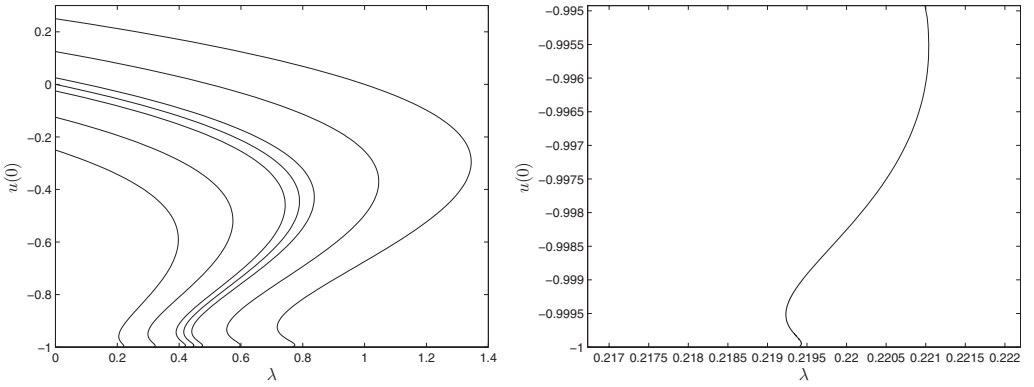

FIGURE 3. (a) Solution curves for various β of boundary value problem (3.4). From left to right, the curves correspond to $\beta = 1, 0.1, 0, -0.1, -1$. (b) A magnified portion of (a), for $\beta = 1$, which begins to show the infinite fold structure (cf. [2]).

$\beta \ll 1$. Since δ and β are both small, their relationship will be resolved in the asymptotic analysis. First, we expand u and the nonlinear eigenvalue parameter λ in the standard way

$$u = u_0 + \beta u_1 + \mathcal{O}(\beta^2), \qquad \lambda = \lambda_0 + \beta\lambda_1 + \mathcal{O}(\beta^2). \tag{3.6}$$

At leading order we take u_0 and λ_0 to be the well-known singular solution

$$u_0(r) = -1 + r^{2/3}, \qquad \lambda_0 = 4/9, \tag{3.7}$$

which implies that there exists a boundary layer at $r = 0$. Then substituting the expansions from (3.6) into (3.4) and equating powers of ε, we find at order $\mathcal{O}(\varepsilon^2)$ that u_1 satisfies

$$u_1'' + \frac{1}{r}u_1' + \frac{2\lambda_0}{r^2}u_1 = \frac{\lambda_1}{r^{4/3}} + 1, \qquad 0 < r < 1; \qquad u_1(1) = 0, \tag{3.8}$$

whose solution is

$$u_1(r) = A_1 \sin\left[\frac{2\sqrt{2}}{3}\log r + \varphi_1\right] + \frac{3\lambda_1}{4}r^{2/3} + \frac{9}{44}r^2; \quad \lambda_1 := -\frac{4A_1}{3}\sin\varphi_1 - \frac{3}{11}. \tag{3.9}$$

Here, A_1 and φ_1 are coefficients due to integration and will be determined via matching.

Near the boundary layer at $r = 0$ we introduce the inner variables

$$u(r) = -1 + \delta w(\rho), \qquad \rho = r/\gamma, \tag{3.10}$$

where $\gamma \ll 1$ is the scale of the boundary layer and is to be determined. Plugging these new variables into boundary value problem (3.4), we obtain the new inner problem

$$w'' + \frac{1}{\rho}w' = \frac{\gamma^2}{\delta^3}\frac{(\lambda_0 + \ldots)}{w^2} + \frac{\gamma^2}{\delta}\beta, \quad 0 < \rho < \infty; \qquad w(0) = 1,\ w'(0) = 0, \tag{3.11}$$

which via a dominant balance implies that $\gamma = \delta^{3/2}$. Then expanding w as $w = w_0$

https://doi.org/10.1017/S0956792512000435 Published online by Cambridge University Press

$+\delta w_1 + \mathcal{O}(\delta)$ and using it in inner problem (3.11), we find that w_0 satisfies the initial value problem

$$w_0'' + \frac{1}{\rho} w_0' = \frac{\lambda_0}{w_0^2}, \quad 0 < \rho < \infty; \qquad w_0(0) = 1, \; w_0'(0) = 0. \tag{3.12}$$

To find the far-field behaviour of w_0 as $\rho \to \infty$, we assume that $w_0 \sim a\,\rho^b$ as $\rho \to \infty$. Plugging this behaviour into (3.12) yields, after a dominant balance

$$a\,b^2 \rho^{b-2} \sim \lambda_0\, a^{-1} \rho^{-2b},$$

hence, $a = 1$ and $b = 2/3$. To find the next order in the far-field behaviour, we let $w_0 \sim \rho^{2/3} + \sigma$, where $\sigma \ll \rho^{2/3}$ as $\rho \to \infty$, and find from initial value problem (3.12) that $\sigma(\rho)$ satisfies the asymptotic differential equation, $\sigma'' + \rho^{-1}\sigma' + 2\lambda_0 \rho^{-2}\sigma \sim 0$ as $\rho \to \infty$, whose solution is

$$\sigma(\rho) \sim \mathsf{A} \sin\left[\frac{2\sqrt{2}}{3}\log\rho + \Phi\right], \quad \text{as } \rho \to \infty.$$

This leads to the following far-field behaviour for the solution w_0 of (3.12):

$$w_0 \sim \rho^{2/3} + \mathsf{A} \sin\left[\frac{2\sqrt{2}}{3}\log\rho + \Phi\right] \quad \text{as } \rho \to \infty. \tag{3.13}$$

Note that here A and Φ must be computed numerically from the solution of initial value problem (3.12) with the asymptotic behaviour given in (3.13). In particular these constants have been computed in [13], and we obtain the same values here: $\mathsf{A} \approx 0.4727$ and $\Phi \approx 3.2110$.

To carry out our matching to $\mathcal{O}(\delta)$, we introduce the intermediate variable $r_\eta = r/\eta(\delta)$, where $\eta \ll 1$ as $\delta \to 0^+$, and the corresponding condition

$$\lim_{\substack{\delta \to 0^+ \\ x_\eta \text{ fixed}}} \frac{1}{\beta}\left[u_0(\eta r_\eta) + \beta u_1(\eta r_\eta) + (1 - \delta w_0(\eta r_\eta/\delta^{3/2}))\right] = 0. \tag{3.14}$$

Using (3.7), (3.9) and (3.13), we obtain

$$\begin{aligned} &u_0(\eta r_\eta) + \beta u_1(\eta r_\eta) + (1 - \delta w_0(\eta r_\eta/\delta^{3/2})) \\ &\quad = \beta A_1 \sin\left[\frac{2\sqrt{2}}{3}\log\eta r_\eta + \varphi_1\right] - \delta\,\mathsf{A}\sin\left[\frac{2\sqrt{2}}{3}\log\eta r_\eta - \sqrt{2}\log\delta + \Phi\right] + \mathcal{O}(\delta), \end{aligned}$$

as $\delta \to 0^+$, for $\delta^{3/2} \ll \eta \ll \delta$. Therefore, for this asymptotic behaviour to vanish as $\delta \to 0^+$, we need $\beta = \mathcal{O}(\delta)$; namely, we let $\beta/\delta = \beta_0$, where $\beta = \mathcal{O}(1)$, and then choose

$$A_1 = \frac{\mathsf{A}}{\beta_0}, \qquad \varphi_1 = \Phi - \sqrt{2}\log\delta, \tag{3.15}$$

so that condition (3.14) is satisfied. Accordingly, we determine from (3.9) that λ_1 is

$$\lambda_1 = -\frac{4\,\mathsf{A}}{3\beta_0}\sin\left[\Phi - \sqrt{2}\log\delta\right] - \frac{3}{11}, \tag{3.16}$$

https://doi.org/10.1017/S0956792512000435 Published online by Cambridge University Press

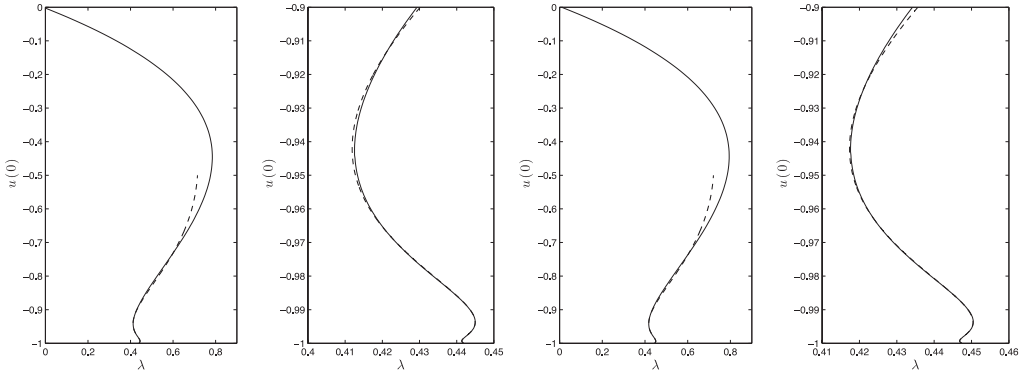

(a) $\beta = 0.01$ (b) $\beta = 0.01$, zoom (c) $\beta = -0.01$ (d) $\beta = -0.01$, zoom

FIGURE 4. (a) For $\beta = 0.01$, a comparison of the solution curve of (3.1) computed numerically (solid) versus its two-term asymptotic approximation (dashed) for the maximal branch given in (3.18). (b) A magnified portion of sub-figure (a). (c) For $\beta = -0.01$, a comparison of the solution curve of (3.1) computed numerically (solid) versus its two-term asymptotic approximation (dashed) for the maximal branch given in (3.18). (d) A magnified portion of sub-figure (c).

and hence

$$\lambda = \frac{4}{9} - \delta\left(\frac{4\,\mathsf{A}}{3}\sin\left[\Phi - \sqrt{2}\log\delta\right] + \frac{3}{11}\beta_0\right) + \mathcal{O}(\delta). \tag{3.17}$$

Next in fixing the value of β in (3.1), and requiring that $\beta_0 = \beta/\delta = \mathcal{O}(1)$, we have the following result for the maximal branch of the solution curve.

Principle Result 3.1 *For $\beta \ll 1$ fixed and $\delta \ll 1$ such that $\beta/\delta = \mathcal{O}(1)$, we have that the two-term asymptotic expansion for the maximal branch of the solution curve for* (3.1) *is given by*

$$u(0) = -1 + \delta, \qquad \lambda = \left(\frac{4}{9} - \frac{3}{11}\beta\right) - \delta\left(\frac{4\,\mathsf{A}}{3}\sin\left[\Phi - \sqrt{2}\log\delta\right]\right) + \mathcal{O}(\delta^2). \tag{3.18}$$

Here, A *and* Φ *are determined from the far-field behaviour*

$$w_0 \sim \rho^{2/3} + \mathsf{A}\sin\left[\frac{2\sqrt{2}}{3}\log\rho + \Phi\right] \quad \text{as} \quad \rho \to \infty,$$

of the initial value problem

$$w_0'' + \frac{1}{\rho}w_0' = \frac{4}{9}w_0^{-2}, \quad 0 < \rho < \infty; \qquad w_0(0) = 1,\ w_0'(0) = 0.$$

In Figure 4, plots of the bifurcation diagram computed numerically are compared to the two-term asymptotic result for the maximal solution branch obtained in (3.18). Here, we can see that the asymptotics closely approximate the numerical results.

https://doi.org/10.1017/S0956792512000435 Published online by Cambridge University Press

3.1.2 *The fold point* $(\lambda^*, u(0))$

In this section, we analyse how λ^* of boundary value problem (3.4) changes with respect to β, for $\beta \ll 1$, via the method outlined by Van De Velde and Ward in [24] (also see [4, 12]). To this end, we assume that the solution curve of boundary value problem (3.4), seen in Figure 3, is given by the graph $(\lambda(\alpha;\beta),\alpha)$, where $\alpha := u(0)$. We denote the fold corresponding to λ^* as $(\lambda^*(\alpha^*,\beta),\alpha^*(\beta))$ and determine it by the following condition:

$$\frac{\mathrm{d}\lambda}{\mathrm{d}\alpha}(\alpha^*) = 0, \tag{3.19}$$

where $\lambda(\alpha^*)$ is a global maximum. Next, since $\beta \ll 1$ and λ and u change with respect to β, we assume that

$$u(r;\alpha,\beta) = u_0(r;\alpha) + \beta u_1(r;\alpha) + \mathcal{O}(\beta^2), \tag{3.20a}$$

$$\lambda(\alpha;\beta) = \lambda_0(\alpha) + \beta\lambda_1(\alpha) + \mathcal{O}(\beta^2). \tag{3.20b}$$

Plugging these expansions into problem (3.4) and equating powers of β, we find that u_0 and u_1 satisfy

$$u_0'' + \frac{1}{r}u_0' = \frac{\lambda_0}{(1+u_0)^2}, \quad 0 < r < 1; \qquad u_0'(0) = 0,\ u_0(1) = 0, \tag{3.21}$$

$$\mathscr{L}u_1 = \frac{\lambda_1}{(1+u_0)^2} + 1, \quad 0 < r < 1; \qquad u_1'(0) = 0,\ u_1(1) = 0, \tag{3.22}$$

where $\mathscr{L}$ is the linear differential operator defined by

$$\mathscr{L}\psi := \psi'' + \frac{1}{r}\psi' + \frac{2\lambda_0}{(1+u_0)^3}\psi. \tag{3.23}$$

We are now setup to determine the asymptotic behaviour of the fold point. First, we expand α^* as $\alpha^*(\beta) = \alpha_0 + \beta\alpha_1 + \cdots$. Then by expanding $\lambda^*(\beta) = \lambda(\alpha^*;\beta)$ for $\beta \ll 1$ and using fold condition (3.19), we find that the two-term expansion for $\lambda^*(\beta)$ is given by

$$\lambda^*(\beta) = \lambda_0(\alpha_0) + \beta\lambda_1(\alpha_0) + \mathcal{O}(\beta^2) \tag{3.24}$$

for $\beta \ll 1$. Next in differentiating expansion (3.20b), evaluating it at $\alpha = \alpha^*(\beta)$ and expanding for small β, we deduce $\mathrm{d}\lambda_0/\mathrm{d}\alpha(\alpha_0) = 0$. This implies that $(\lambda_0(\alpha_0),\alpha_0)$ is exactly the fold point corresponding to λ^* of the unperturbed problem; hence, $\lambda_0(\alpha_0) \approx 0.7892$ and all we need to find is $\lambda_1(\alpha_0)$.

To do so, we notice that for our asymptotic expansion to be valid, we need a unique solution at $\mathcal{O}(\beta)$; more precisely, we need a unique solution for $\alpha = \alpha_0$. However, differentiating the problem (3.22) with respect to α and then evaluating it at $\alpha = \alpha_0$ gives

$$\mathscr{L}\left[\frac{\partial u_0}{\partial\alpha}(\,\cdot\,;\alpha_0)\right] = 0.$$

Thus, $\partial_\alpha u_0|_{\alpha=\alpha_0}$ is a nontrivial solution to homogeneous version of boundary value problem (3.22), and by the Fredholm solvability condition, we need $\partial_\alpha u_0|_{\alpha=\alpha_0}$ to be orthogonal in

https://doi.org/10.1017/S0956792512000435 Published online by Cambridge University Press

the sense of L^2 to the right-hand side of (3.22) at $\alpha = \alpha_0$

$$\int_0^1 \frac{\partial u_0}{\partial \alpha}(r;\alpha_0)\left[\frac{\lambda_1(\alpha_0)}{(1+u_0(r;\alpha_0))^2}+1\right] r\,\mathrm{d}r = 0.$$

Finally in using this solvability condition to find $\lambda_1(\alpha_0)$, we have the following asymptotic result for λ^* of problem (3.4).

Principle Result 3.2 *Assume $\beta \ll 1$. If (λ_0, α_0) is the fold point corresponding to λ^* of unperturbed problem* (3.21)*, then the two-term asymptotic expansion for λ^* of* (3.4) *is given by*

$$\lambda^*(\beta) = \lambda_0 + \beta\lambda_g + \mathcal{O}(\beta^2), \qquad \lambda_g := -\frac{\int_0^1 \varphi\, r\,\mathrm{d}r}{\int_0^1 \varphi(1+u_0)^{-2}\, r\,\mathrm{d}r}, \tag{3.25 a, b}$$

where u_0 satisfies (3.21) *with $u_0(0) = \alpha_0$ and φ satisfies*

$$\varphi'' + \frac{1}{r}\varphi' + \frac{2\lambda_0}{(1+u_0)^3}\varphi = 0, \quad 0 < r < 1; \qquad \varphi'(0) = 0,\ \varphi(1) = 0,$$

such that $\|\varphi\|_\infty = 1$. Note that here the subscript g is used because the correction is due to the effect of gravity.

Thus, using definition (3.25 *b*) to calculate that $\lambda_g \approx -0.4709$, we have the following explicit two-term expansion for λ^* of (3.4), which is valid for $\beta \ll 1$:

$$\lambda^*(\beta) \sim 0.7892 - 0.4709\beta. \tag{3.26}$$

Figure 5 provides a comparison of the computed two-term asymptotic approximation, (3.25 *a*), versus the full numerical approximation of λ^*. It is observed that even out to $|\beta| = 0.25$ the agreement is very good.

4 The effects of gravity and curvature

In this section, we investigate the effects of gravity and curvature on the λ^*. First, since physically $0 < \varepsilon^2 \ll 1$ and $\beta \ll 1$, we drop the order $\mathcal{O}(\varepsilon^2\beta)$ terms in boundary value problem (2.5) and study the resulting model for the shape u of the deflected elastic membrane

$$\operatorname{div}\frac{\nabla u}{\sqrt{1+\varepsilon^2|\nabla u|^2}} = \frac{\lambda}{(1+u)^2} + \beta \quad \text{in} \quad \Omega, \qquad u = 0 \quad \text{in} \quad \partial\Omega. \tag{4.1}$$

(Note that this boundary value problem is very similar to the one studied by Mellet and Vovelle in [14]; however, the nonlinear forcing term is slightly different.) To ensure that this model captures the proper behaviour of the system, we first show that there exists a λ^* for boundary value problem (4.1). However, this takes some care and we consider two separate cases: $\beta \geqslant 0$ and $\beta < 0$.

First for $\beta \geqslant 0$ we have the following proposition that follows easily from comparison principles for nonlinear, elliptic operators (see, e.g. Theorem 31 of Ch. 2 in [21]).

https://doi.org/10.1017/S0956792512000435 Published online by Cambridge University Press

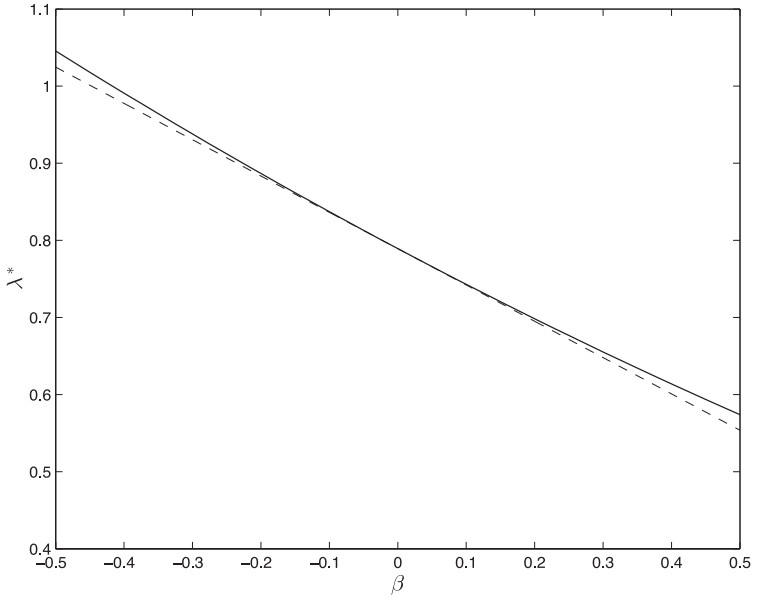

FIGURE 5. The two-term asymptotic approximation of λ^* for boundary value problem (3.4) given in (3.25) (dashed) versus the full numerical approximation (line).

Proposition 4.1 *Assume that* $\beta \geqslant 0$ *and* $\lambda \geqslant 0$. *If* u *in* $C^2(\Omega) \cap C(\bar{\Omega})$ *is a solution of* (4.1), *then* $u(x) \leqslant 0$ *for* x *in* Ω.

With this result, we may prove the following.

Lemma 4.2 *Let* $\varepsilon > 0$, $\beta \geqslant 0$ *and* $\lambda \geqslant 0$. *Then there exist two values* λ^* *and* β^* *such that if* $\lambda > \lambda^*$ *or* $\beta > \beta^*$, *no solutions of* (4.1) *exist; furthermore, we have the following estimates:*

$$\lambda^* \leqslant \min\left\{\frac{1}{\varepsilon}\frac{|\partial\Omega|}{|\Omega|} - \beta, \frac{4\kappa_1}{27}\right\} \qquad \text{and} \qquad \beta^* \leqslant \min\left\{\frac{1}{\varepsilon}\frac{|\partial\Omega|}{|\Omega|}, \kappa_1\right\}, \tag{4.2}$$

where κ_1 *is the first eigenvalue of* $-\Delta$ *on* Ω *with homogeneous Dirichlet boundary conditions.*

Proof Integrating the partial differential equation given in problem (4.1) over Ω and using the divergence theorem, we obtain

$$\int_{\partial\Omega} \frac{\nabla u \cdot v}{\sqrt{1+\varepsilon^2|\nabla u|^2}}\,\mathrm{d}s = \lambda \int_\Omega (1+u)^{-2}\,\mathrm{d}x + \beta|\Omega|, \tag{4.3}$$

where v is the exterior unit normal vector of Ω; hence

$$\lambda \int_\Omega (1+u)^{-2}\,\mathrm{d}x + \beta|\Omega| \leqslant \left|\int_{\partial\Omega} \frac{\nabla u \cdot v}{\sqrt{1+\varepsilon^2|\nabla u|^2}}\,\mathrm{d}s\right| \leqslant \int_{\partial\Omega} \frac{|\nabla u \cdot v|}{\sqrt{1+\varepsilon^2|\nabla u|^2}}\,\mathrm{d}s,$$

https://doi.org/10.1017/S0956792512000435 Published online by Cambridge University Press

which, by the Cauchy–Schwarz inequality and $|v| = 1$, implies

$$\lambda \int_\Omega (1+u)^{-2}\,\mathrm{d}x + \beta|\Omega| \leqslant \int_{\partial\Omega} \frac{|\nabla u|}{\sqrt{1+\varepsilon^2|\nabla u|^2}}\,\mathrm{d}s. \tag{4.4}$$

Next observe that

$$\lambda|\Omega| \leqslant \lambda \int_\Omega (1+u)^{-2}\,\mathrm{d}x; \qquad \frac{|\nabla u|}{\sqrt{1+\varepsilon^2|\nabla u|^2}} \leqslant 1, \tag{4.5 a, b}$$

where inequality (4.5 *a*) comes from Proposition 4.1. By using these inequalities in (4.4) we obtain $\lambda|\Omega| + \beta|\Omega| \leqslant |\partial\Omega|/\varepsilon$, which implies that $\lambda \leqslant |\partial\Omega|/\varepsilon|\Omega| - \beta$ and $\beta \leqslant |\partial\Omega|/\varepsilon|\Omega|$.

To get the other bounds we let u be a solution of (4.1) and consider the eigenvalue problem

$$-\operatorname{div} \frac{\nabla\varphi}{\sqrt{1+\varepsilon^2|\nabla u|^2}} = \mu\varphi \quad \text{in} \quad \Omega; \qquad \varphi = 0 \quad \text{on} \quad \Omega, \tag{4.6}$$

for φ in $H_0^1(\Omega)$. First in multiplying the partial differential equations in problems (4.1) and (4.6) by φ and u, respectively, and integrating over Ω, we obtain

$$-\int_\Omega \frac{\nabla\varphi\cdot\nabla u}{\sqrt{1+\varepsilon^2|\nabla u|^2}}\,\mathrm{d}x = \int_\Omega \left[\frac{\lambda}{(1+u)^2} + \beta\right]\varphi\,\mathrm{d}x; \quad \int_\Omega \frac{\nabla\varphi\cdot\nabla u}{\sqrt{1+\varepsilon^2|\nabla u|^2}}\,\mathrm{d}x = \int_\Omega \mu\varphi u\,\mathrm{d}x.$$

Then adding these equations yields the following solvability condition for u:

$$\int_\Omega \left(\mu u + \frac{\lambda}{(1+u)^2} + \beta\right)\varphi\,\mathrm{d}x = 0, \tag{4.7}$$

for all eigenpairs (μ, φ) of problem (4.6). In particular, condition (4.7) holds for the first eigenvalue μ_1 of problem (4.6) (which is positive and simple) and its corresponding eigenvector φ_1, which can – and will – be chosen to be strictly positive in Ω (see, e.g. Theorem 8.38 of [9]). Therefore, with $\phi_1 > 0$ in condition (4.7), the term $\mu_1 u + \lambda(1+u)^{-2} + \beta$ must be identically zero or change sign. It is clear that it is not zero, so there must be a value of u in $(-1, 0)$, say $\hat{u}$, where $\lambda(1+\hat{u})^{-2} = -\mu_1\hat{u} - \beta$. Consequently

$$\lambda \leqslant \frac{4}{27}\frac{(\mu_1 - \beta)^3}{\mu_1^2}.$$

Then since $\lambda \geqslant 0$, we deduce that $\beta \leqslant \mu_1$ and $\lambda \leqslant (4\mu_1)/27$. However, by Rayleigh's formula, we also have

$$\begin{aligned}\mu_1 &= \inf\left\{\int_\Omega \frac{|\nabla\varphi|^2}{\sqrt{1+\varepsilon^2|\nabla u|^2}}\,\mathrm{d}x : \varphi \in H_0^1(\Omega),\ \|\varphi\|_{L^2(\Omega)} = 1\right\}\\ &\leqslant \inf\left\{\int_\Omega |\nabla\varphi|^2\,\mathrm{d}x : \varphi \in H_0^1(\Omega),\ \|\varphi\|_{L^2(\Omega)} = 1\right\}\\ &= \kappa_1,\end{aligned}$$

where κ_1 is the first eigenvalue of $-\Delta$ on Ω with homogeneous Dirichlet boundary conditions. Therefore, $0 \leqslant \lambda \leqslant (4/27)\kappa_1$ and $\beta \leqslant \kappa_1$.

https://doi.org/10.1017/S0956792512000435 Published online by Cambridge University Press

In collecting our results we have that if u is a solution of (4.1)

$$\lambda \leqslant \min\left\{\frac{1}{\varepsilon}\frac{|\partial\Omega|}{|\Omega|} - \beta, \frac{4\kappa_1}{27}\right\} \qquad \text{and} \qquad \beta \leqslant \min\left\{\frac{1}{\varepsilon}\frac{|\partial\Omega|}{|\Omega|}, \kappa_1\right\}.$$

In taking the contrapositive we obtain our result desired result. □

Second, for $\beta < 0$, we impose the constraint $\beta \geqslant -2/\varepsilon$. While this does not require that $\beta \ll 1$ when $\varepsilon \ll 1$ (which is a physical requirement), it does capture that regime and provides for more generality. From these assumptions we can also prove the existence of a λ^*.

Proposition 4.3 *Assume that $\varepsilon > 0$, $\beta \in [-2/\varepsilon, 0)$ and $\lambda \geqslant 0$. If u in $C^2(\Omega) \cap C(\bar{\Omega})$ is a solution of boundary value problem* (4.1)*, then $u(x) \leqslant M := \sqrt{4 - \varepsilon^2\beta^2}/(\beta\varepsilon^2)$, for x in Ω.*

Proof Note that from the definition of the dimensionless parameters (2.2), $\Omega \subseteq \mathscr{D}_1$, where $\mathscr{D}_1$ is the unit disk in $\mathbb{R}^2$ whose centre is at the origin. Next observe that for β in $[-2/\varepsilon, 0)$, the function w defined by

$$w(x) := \frac{\sqrt{4 - \varepsilon^2\beta^2} - \sqrt{4 - \varepsilon^2\beta^2|x|^2}}{\varepsilon^2\beta}$$

is a solution of

$$\operatorname{div}\frac{\nabla w}{\sqrt{1 + \varepsilon^2|\nabla w|^2}} = \beta \quad \text{in} \quad \mathscr{D}_1.$$

Furthermore, $w \geqslant 0$ in $\mathscr{D}_1$, which implies that $w \geqslant 0$ on $\partial\Omega$; therefore, if u is a solution of (4.1), then

$$\operatorname{div}\frac{\nabla u}{\sqrt{1 + \varepsilon^2|\nabla u|^2}} \geqslant \operatorname{div}\frac{\nabla w}{\sqrt{1 + \varepsilon^2|\nabla w|^2}}, \quad \text{in} \quad \Omega; \qquad w \geqslant u \quad \text{on} \quad \partial\Omega,$$

which implies by the comparison principle for nonlinear, elliptic operators (see, e.g. Ch. 2, Thm. 31 of [21]) that $u(x) \leqslant \max_{x\in\Omega} w(x) = \sqrt{4 - \varepsilon^2\beta^2}/(\varepsilon^2\beta)$. □

Lemma 4.4 *Assume $\varepsilon > 0$, $\beta \in [-2/\varepsilon, 0)$ and $\lambda \geqslant 0$. Then there exists a value λ^* such that for all $\lambda > \lambda^*$, no solutions of boundary value problem* (4.1) *exist; furthermore*

$$\lambda^* \leqslant \left[\frac{1}{\varepsilon}\frac{|\partial\Omega|}{|\Omega|} - \beta\right](1 + M)^2, \tag{4.8}$$

where $M = \sqrt{4 - \varepsilon^2\beta^2}/(\beta\varepsilon^2)$.

Proof This proof follows essentially the same as the first part of Lemma 4.2, except from Proposition 4.3 we have that inequality (4.5 *a*) must be replaced by

$$\frac{\lambda|\Omega|}{(1 + M)^2} \leqslant \int_\Omega \frac{\lambda}{(1 + u)^2}\,\mathrm{d}x.$$

□

https://doi.org/10.1017/S0956792512000435 Published online by Cambridge University Press

Thus, in combining Lemmas 4.2 and 4.4, we have the following theorem about the existence of a λ^*.

Theorem 4.5 *For all $\varepsilon > 0$ and $\beta \geqslant -2/\varepsilon$, there exists a value λ^* such that for all $\lambda > \lambda^*$, no solutions of problem* (4.1) *exist.*

Now that we have established the existence of a λ^*, we explore how it varies with respect to ε and β. With the opportunity for comparison to our previous analysis, we look at the special case where Ω is the unit disk $\mathscr{D}_1$. Again by Theorem 1 of [8], if $\beta \leqslant 0$, then solutions of (4.1) must have radial symmetry and boundary value problem (4.1) becomes

$$\frac{1}{r}\left(\frac{ru'}{\sqrt{1+\varepsilon^2(u')^2}}\right)' = \frac{\lambda}{(1+u)^2} + \beta, \quad 0 < r < 1; \quad u'(0) = 0,\ u(1) = 0. \tag{4.9}$$

Here $r = |x|$ and $u(x) = u(r)$. If $\beta < 0$, this is not necessarily true. However, for simplicity we only look for radial solutions of (4.9) in this situation as well. Using the same shooting method as before we can compute the bifurcation diagrams, shown in Figure 6, for various ε and β. From these diagrams, we observe the following.

One, when $\varepsilon \neq 0$, the solution curves stop at some finite value before reaching $u(0) = -1$. This ending point occurs when the derivative of solution becomes singular for some r in $(0, 1)$, which is similar to the case for $\beta = 0$ and $\varepsilon \neq 0$ and seemingly can be made rigorous with the same approach (cf. [3]). Note that this disappearance of solutions is similar to the behaviour of other mean curvature type equations (cf. [4], [15], [16]).

Two, for small $\varepsilon \ll 1$, a second solution branch appears for $\beta \approx -18$ and $\lambda \ll 1$ (see Figure 7). Initially this new branch is isolated from the main branch and has one saddle node bifurcation. Then as β is increased this new branch's saddle node coalesces with the second fold of the main solution branch. In the next section, we analyse the appearance of this new branch using formal asymptotics, before moving on to the dynamics of λ^* with respect to small ε and β.

4.1 Appearance of a new solution branch

To find the new solution branch, we look at problem (4.9) in the limit $\delta = 1 + u(r_c) \to 0^+$. Here r_c is a critical point of u that corresponds to a local minimum and is to be determined. With this restriction, we assume that u, λ and r_c have the following naïve regular expansions:

$$u = u_0 + \delta u_1 + \cdots, \quad \lambda = \delta\lambda_0 + \cdots, \quad r_c = r_0 + \cdots, \tag{4.10a,b,c}$$

as $\delta \to 0^+$. From plugging these expansions into (4.9), we find that u_0 and u_1 satisfy

$$\frac{1}{r}\left(\frac{ru_0'}{\sqrt{1+\varepsilon^2(u_0')^2}}\right)' = \beta, \qquad 0 < r < 1; \qquad u_0'(0) = u_0(1) = 0, \tag{4.11a}$$

$$\mathscr{L}u_1 = \frac{\lambda_0}{(1+u_0)^2}, \qquad 0 < r < 1; \qquad u_1'(0) = u_1(1) = 0, \tag{4.11b}$$

https://doi.org/10.1017/S0956792512000435 Published online by Cambridge University Press

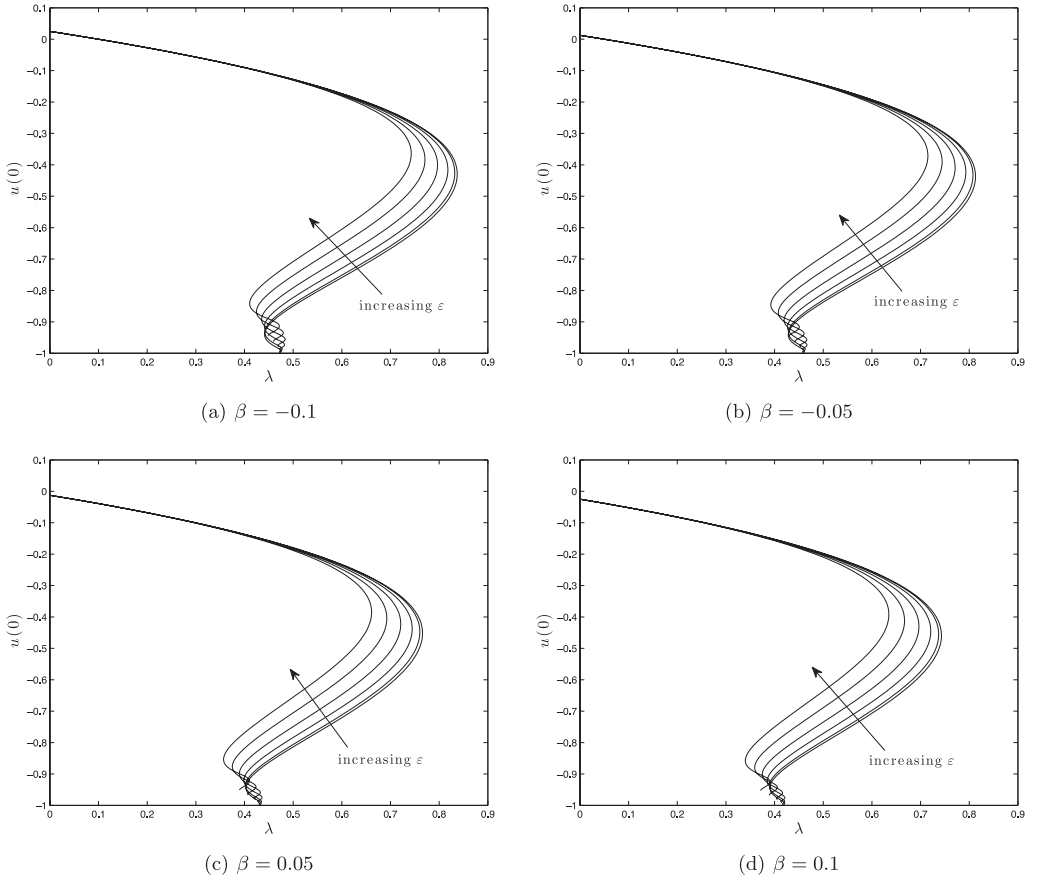

(a) $\beta = -0.1$ (b) $\beta = -0.05$

(c) $\beta = 0.05$ (d) $\beta = 0.1$

FIGURE 6. Solution curves of (4.9). (a) Fixed $\beta = 0.1$ and $\varepsilon = 0, 0.2, 0.4, 0.6, 0.8, 1$. (b) Fixed $\beta = -0.1$ and $\varepsilon = 0, 0.4, 0.8, 1.2, 1.6, 2$. (c) Fixed $\beta = 1$ and $\varepsilon = 0, 0.2, 0.4, 0.6, 0.8, 1$. (d) Fixed $\beta = -1$ and $\varepsilon = 0, 0.2, 0.4, 0.6, 0.8, 1$.

respectively. Here, the differential operator $\mathscr{L}$ is defined by

$$\mathscr{L}\varphi := \frac{1}{r}\left(\frac{r\varphi'}{\left(1+\varepsilon^2(u_0')^2\right)^{3/2}}\right)'. \tag{4.12}$$

Upon solving the ordinary differential equation given in (4.11*a*), we find that its general solutions are given by

$$f(r) = A_0^- + \frac{\sqrt{4-\varepsilon^2\beta^2 r^2}-2}{\varepsilon^2\beta}, \quad g(r) = \int_1^r \frac{\beta z^2 + A_0^+}{\sqrt{4z^2 - \varepsilon^2(\beta z^2 + A_0^+)^2}}\,\mathrm{d}z, \tag{4.13 a, b}$$

where f and g correspond to applying the boundary conditions $u_0'(0) = 0$ and $u_0(1) = 0$, respectively. In particular, $A_0^- := u_0(0)$ and $A_0^+ := 2u_0'(1)/\sqrt{1+\varepsilon^2 u_0'(1)^2} - \beta$. By piecing

https://doi.org/10.1017/S0956792512000435 Published online by Cambridge University Press

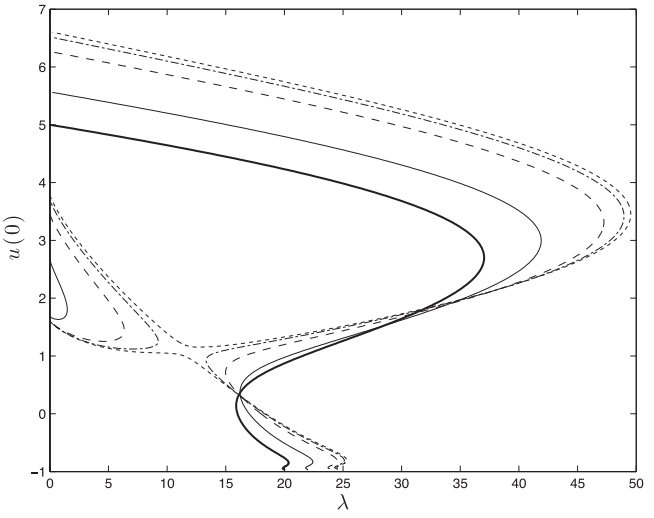

FIGURE 7. Solution curves of (4.9) for $\varepsilon = 0.1$ and $\beta = -16$ (thick line), -17 (line), -18 (dashed), -18.3 (dot-dashed) and -18.4 (dotted). Note that for $\beta = -16$, there is only on curve. Then for $\beta = -17$, the second solution curve appears small λ and $u(0) \approx 2$. Also as β increases from -18.3 to -18.4, the saddle node of the new branch and the second fold of the old branch approach, touch and then move away with new bifurcation structure.

these solutions together and applying the point constraint $u(r_0) = -1$, we find that the leading order outer solution u_0 is given by the piecewise function

$$u_0(r) := \begin{cases} -1 + \dfrac{\sqrt{4 - \varepsilon^2\beta^2 r_0^2} - \sqrt{4 - \varepsilon^2\beta^2 r^2}}{\varepsilon^2\beta}, & 0 < r \leqslant r_0, \\ \displaystyle\int_1^r \frac{\beta z^2 + A_0^+}{\sqrt{4z^2 - \varepsilon^2(\beta z^2 + A_0^+)^2}}\,\mathrm{d}z, & r_0 < r < 1, \end{cases} \tag{4.14}$$

where

$$\int_{r_0}^1 \frac{\beta z^2 + A_0^+}{\sqrt{4z^2 - \varepsilon^2(\beta z^2 + A_0^+)^2}}\,\mathrm{d}z = 1. \tag{4.15}$$

From this we see that u_0 is not differentiable at r_0, indicating the presence of an interior layer. Also since $u_0 \sim -1 + u_0'(r_0^\pm)(r - r_0) + (1/2)u_0''(r_0^\pm)(r - r_0)^2$ as $r \to r_0^\pm$, we have that u_1 satisfies the asymptotic differential equation

$$\mathscr{L}u_1 \sim \frac{\lambda_0 r_0}{u_0'(r_0^\pm)^2}(r - r_0)^{-2} + \frac{\lambda_0(u_0'(r_0^\pm) - r_0 u_0''(r_0^\pm))}{u_0'(r_0^\pm)^3}(r - r_0)^{-1},$$

https://doi.org/10.1017/S0956792512000435 Published online by Cambridge University Press

as $r \to r_0^{\pm}$. This gives the limiting behaviour

$$u_1 = -\frac{\lambda_0\left(1+\varepsilon^2 {u_0}'(r_0^{\pm})^2\right)^{3/2}}{{u_0}'(r_0^{\pm})^2}\log|r-r_0| + A_1^{\pm} + \frac{\lambda_0\left(1+\varepsilon^2 {u_0}'(r_0^{\pm})^2\right)^{3/2}\left({u_0}'(r_0^{\pm}) - r_0 {u_0}''(r_0^{\pm})\right)}{r_0 {u_0}'(r_0^{\pm})^3}(r-r_0)\log|r-r_0| + \mathcal{O}(r-r_0),$$

as $r \to r_0^{\pm}$. Here, $u_0^{(n)}(r_0^{\pm}) := \lim_{r\to r_0^{\pm}} u_0^{(n)}(r)$ and $A_1^{\pm}$ are constants associated with the homogeneous solution of (4.11*b*) that will be determined from matching.

In the interior layer, we introduce the variables inner variables

$$\rho = (r-r_0)/\mu, \qquad u(r) = -1 + \delta v(\rho), \tag{4.16 a, b}$$

where $\mu(\delta) \ll 1$ – the width of the layer – is to be determined. To do so, we begin by writing the leading order outer solution in terms of the the inner variable: $u \sim -1 + \mu {u_0}'(r_0^{\pm})\rho$ as $r \to r_0^{\pm}$; hence, in comparing this asymptotic behaviour with the equation (4.16 *b*), we find $\mu = \delta$. Then using (4.16) in (4.9) we find that the full inner differential equation for v is given by

$$\left(\frac{v'}{\sqrt{1+\varepsilon^2(v')^2}}\right)' + \frac{\delta}{r_0+\delta\rho}\frac{v'}{\sqrt{1+\varepsilon^2(v')^2}} = \frac{v}{\delta}\frac{(\lambda_0+\mathcal{o}(1))}{v^2} + \delta\beta. \tag{4.17a}$$

A dominant balance reveals that v scales like δ, i.e. $v = \delta$. Letting $r = r_c$ in (4.16), the corresponding initial conditions become

$$v(\rho_c) = 1, \qquad v'(\rho_c) = 0, \tag{4.17b}$$

where $\rho_c = (r_c - r_0)/\delta$. Thus, in expanding v as $v \sim v_0$ the leading order inner problem becomes

$$\left(\frac{{v_0}'}{\sqrt{1+\varepsilon^2({v_0}')^2}}\right)' = \frac{\lambda_0}{{v_0}^2}, \quad -\infty < \rho < \infty; \qquad v_0(0) = 1,\ {v_0}'(0) = 0, \tag{4.18}$$

where we have also used (4.10 *c*). For the far-field behaviour of this differential equation, we prove the following.

Proposition 4.6 *For classical solutions of* (4.18) *to exist, it is necessary that* $\lambda_0 > \varepsilon^2$. *Also for fixed* λ_0, *the solution* v_0 *of* (4.18) *(if it exists) is unique and goes to* $+\infty$ *as* $\rho \to +\infty$; *specifically*

$$|\rho| = \frac{\varepsilon^3 E}{\sqrt{1-\varepsilon^4E^2}}v_0 + \frac{\varepsilon^3\lambda_0\log v_0}{(1-\varepsilon^4E^2)^{3/2}} - \frac{\varepsilon^3\chi}{\left(1-\varepsilon^4E^2\right)^{3/2}} + \mathcal{O}({v_0}^{-1}), \quad v_0 \to +\infty, \tag{4.19}$$

where χ *is defined in* (4.21) *and* $E := \varepsilon^{-2} - \lambda_0$.

https://doi.org/10.1017/S0956792512000435 Published online by Cambridge University Press

Proof Note that uniqueness of v_0 follows from standard methods (see, e.g. [6]). First by carrying out the differentiation in (4.18), we find that

$$v_0''(\rho) = \lambda_0 \frac{(1+\varepsilon^2 v_0'(\rho)^2)^{3/2}}{v_0(\rho)^2},$$

so that $\operatorname{sgn}(v_0'') = \operatorname{sgn}(\lambda_0)$ for all ρ in $(-\infty, \infty)$; however, $\operatorname{sgn}(\lambda_0)$ cannot be negative because the right-hand side of the differential equation will blow-up. Therefore, λ_0 must be positive, and consequently, $v_0'' > 0$ for all ρ in $(-\infty, \infty)$. This implies that $v_0 > 0$ for all ρ and cannot be bounded from above. It is also easy to see that (4.18) has the following first integral:

$$\frac{1}{\varepsilon^2\sqrt{1+\varepsilon^2(v_0')^2}} - \frac{\lambda_0}{v_0} = E := \frac{1}{\varepsilon^2} - \lambda_0, \qquad -\infty < \rho < \infty. \tag{4.20}$$

Because the first term on the left-hand side is positive, $\lambda_0 v_0^{-1} + E > 0$ for all ρ. Consequently since v_0 cannot be bounded from above, we must have $E > 0$, namely, $\lambda_0 > \varepsilon^2$. Solving for v_0' in (4.20) gives

$$v_0'(\rho) = \begin{cases} -\dfrac{\sqrt{v_0^2 - \varepsilon^4(\lambda_0 + Ev_0)^2}}{\varepsilon^3(\lambda_0 + Ev_0)}, & -\infty < \rho < 0, \\ \dfrac{\sqrt{v_0^2 - \varepsilon^4(\lambda_0 + Ev_0)^2}}{\varepsilon^3(\lambda_0 + Ev_0)}, & 0 < \rho < \infty. \end{cases}$$

Finally in separating variables and integrating, we have

$$\begin{aligned} \rho &= \varepsilon^3 \int_{v_0}^{1} \frac{(\lambda_0 + Ez)}{\sqrt{z^2 - \varepsilon^4(\lambda_0 + Ez)^2}}\,\mathrm{d}z \\ &= -\frac{\varepsilon^3 E}{\sqrt{1-\varepsilon^4E^2}} v_0 - \frac{\varepsilon^3\lambda_0 \log v_0}{(1-\varepsilon^4E^2)^{3/2}} + \frac{\varepsilon^3\chi}{\left(1-\varepsilon^4E^2\right)^{3/2}} + \mathcal{O}(v_0^{-1}), \end{aligned}$$

as $v_0 \to \infty$, for $\rho < 0$, where

$$\begin{aligned} \chi := {} & E\sqrt{1-\varepsilon^4E^2}\sqrt{1-\varepsilon^4(\lambda_0+E)^2} + \lambda_0\varepsilon^4E^2 - \lambda_0 \log\left[2(1-\varepsilon^4E^2)\right] \\ & + \lambda_0 \log\left[1 - \varepsilon^4E(\lambda_0+E) + \sqrt{1-\varepsilon^4E^2}\sqrt{1-\varepsilon^4(\lambda_0+E)^2}\right]. \end{aligned} \tag{4.21}$$

Similarly, we have

$$\begin{aligned} \rho &= \varepsilon^3 \int_{1}^{v_0} \frac{(\lambda_0 + Ez)}{\sqrt{z^2 - \varepsilon^4(\lambda_0 + Ez)^2}}\,\mathrm{d}z \\ &= \frac{\varepsilon^3 E}{\sqrt{1-\varepsilon^4E^2}} v_0 + \frac{\varepsilon^3\lambda_0 \log v_0}{(1-\varepsilon^4E^2)^{3/2}} - \frac{\varepsilon^3\chi}{\left(1-\varepsilon^4E^2\right)^{3/2}} + \mathcal{O}(v_0^{-1}), \end{aligned}$$

as $v_0 \to \infty$, for $\rho > 0$. □

https://doi.org/10.1017/S0956792512000435 Published online by Cambridge University Press

Using series reversion on (4.19) and plugging the result into the inner dependent variable (4.16*b*) we have that

$$u = -1 + \delta\left[\frac{\sqrt{1-\varepsilon^4E^2}}{\varepsilon^3E}|\rho| - \frac{\lambda_0}{E\left(1-\varepsilon^4E^2\right)}\log|\rho| + \frac{1}{E\left(1-\varepsilon^4E^2\right)}\left(\chi - \lambda_0\log\frac{\sqrt{1-\varepsilon^4E^2}}{\varepsilon^3E}\right)\right] + \mathcal{o}(\delta), \tag{4.22}$$

as $|\rho| \to \infty$. For matching we next write the outer solution in terms of the inner variable:

$$u = -1 + (-\delta\log\delta)\frac{\lambda_0\left(1+\varepsilon^2{u_0}'(r_0^{\pm})^2\right)^{3/2}}{{u_0}'(r_0^{\pm})^2} + \delta\left[{u_0}'(r_0^{\pm})\rho - \frac{\lambda_0\left(1+\varepsilon^2{u_0}'(r_0^{\pm})^2\right)^{3/2}}{{u_0}'(r_0^{\pm})^2}\log|\rho| + A_1^{\pm}\right] + \mathcal{o}(\delta), \tag{4.23}$$

as $r \to r_0^{\pm}$; however in comparing (4.22) and (4.23), we see that the order $\mathcal{O}(\delta\log\delta)$ term cannot be removed. Consequently, we must modify our expansion for u given in (4.10*a*) to include a switchback term:

$$u = u_0 + (-\delta\log\delta)u_{1/2} + \delta u_1 + \mathcal{o}(\delta), \tag{4.24}$$

as $\delta \to 0^+$. Therefore using (4.24) in (4.9), we find that

$$\mathscr{L}u_{1/2} = 0, \quad 0 < r < r_0, \quad r_0 < r < 1; \qquad {u_{1/2}}'(0) = u_{1/2}(1) = 0, \tag{4.25}$$

whose solution is given by

$$u_{1/2}(r) = \begin{cases} A_{1/2}^-, & 0 < r \leqslant r_0, \\ A_{1/2}^+\displaystyle\int_r^1 \frac{(1+\varepsilon^2{u_0}'(z)^2)^{3/2}}{z}\,\mathrm{d}z, & r_0 < r < 1. \end{cases}$$

Here, $A_{1/2}^-$ and $A_{1/2}^+$ will be chosen to get rid of the $\mathcal{O}(\delta\log\delta)$ term in (4.23); namely

$$A_{1/2}^- = -\frac{\lambda_0\left(1+\varepsilon^2{u_0}'(r_0^-)^2\right)^{3/2}}{{u_0}'(r_0^-)^2}, \qquad A_{1/2}^+ = -\frac{\lambda_0\left(1+\varepsilon^2{u_0}'(r_0^+)^2\right)^{3/2}}{{u_0}'(r_0^+)^2}\left[\int_{r_0}^1 \frac{(1+\varepsilon^2{u_0}'(z)^2)^{3/2}}{z}\,\mathrm{d}z\right]^{-1}. \tag{4.26}$$

Then in using these switchback terms we have that (4.23) becomes

$$u = -1 + \delta\left[{u_0}'(r_0^{\pm})\rho - \frac{\left(1+\varepsilon^2{u_0}'(r_0^{\pm})^2\right)^{3/2}}{{u_0}'(r_0^{\pm})^2}\log|\rho| + A_1^{\pm}\right] + \mathcal{o}(\delta), \tag{4.27}$$

https://doi.org/10.1017/S0956792512000435 Published online by Cambridge University Press

as $r \to r_0^{\pm}$. Finally by requiring that asymptotic equations (4.22) and (4.27) match, we deduce

$$u_0'(r_0^{\pm}) = \pm\frac{\sqrt{1-\varepsilon^4E^2}}{\varepsilon^3 E}, \qquad A_1^{\pm} = \frac{\chi - \lambda_0 \log(\sqrt{1-\varepsilon^4E^2}/\varepsilon^3 E)}{E\left(1-\varepsilon^4E^2\right)}. \tag{4.28 a, b}$$

Note that (4.28a) gives two equations that yield

$$A_0^{+} = -2\beta {r_0}^2, \qquad \lambda_0 = \frac{2-\sqrt{4-\varepsilon^2\beta^2{r_0}^2}}{2\varepsilon^2}, \tag{4.29 a, b}$$

and all that is left to determine is r_0 from equation (4.15):

$$I(r_0;\beta,\varepsilon) := \beta\int_{r_0}^{1} \frac{z^2-2{r_0}^2}{\sqrt{4z^2-\varepsilon^2\beta^2(z^2-2{r_0}^2)^2}}\,\mathrm{d}z = 1. \tag{4.30a}$$

As a result, we find that a new solution branch of (4.9) will appear if the function $I(r_0;\beta,\varepsilon)-1$ has a zero in $(0,1)$. To find when first happens, we supplement (4.30a) with $\partial I/\partial R = 0$. That is

$$\frac{\beta r_0}{\sqrt{4-\varepsilon^2\beta^2{r_0}^2}} + \int_{r_0}^{1} \frac{\partial}{\partial r_0}\left[\frac{\beta z^2 - 2\beta {r_0}^2}{\sqrt{4z^2-\varepsilon^2\beta^2\left(z^2-2{r_0}^2\right)^2}}\right]\mathrm{d}z = 0. \tag{4.30b}$$

Finally to find the asymptotic approximation for the first solution (β, r_0) of system (4.30) for $\varepsilon \ll 1$, we expand β and r_0 as $\beta \sim \beta_0 + \varepsilon^2\beta_1$ and $r_0 \sim r_{00} + \varepsilon^2 r_{01}$. Solving out to $\mathcal{O}(\varepsilon^2)$ yields

$$\beta \sim \frac{4\sqrt{e}}{\sqrt{e}-2} - \varepsilon^2\frac{4\sqrt{e}\left(16+7\sqrt{e}-12e+e^{3/2}\right)}{\left(\sqrt{e}-2\right)^4}, \quad r_0 \sim e^{-1/4} + \varepsilon^2\frac{5\sqrt{e}+6e-24}{2\left(\sqrt{e}-2\right)^2\sqrt[4]{e}}.$$

Therefore, for small $\varepsilon \ll 1$ the second solution branch of problem (4.9) appears when $\beta \approx -18.7739 + 258.413\varepsilon^2$. The appearance of this new branch is similar to what happens when $\varepsilon = 0$ (cf. [[2], §3.4.2.4]). Also we expect more solution branches to appear as β becomes very large since this analysis can be repeated for more piecewise outer solutions like (4.14). However, since $\beta \gg 1$ is not a physically valid regime, we do not proceed any further.

4.2 Asymptotic analysis of λ^*

In this section, we use the same technique as in Section 3.1.2 to investigate the behaviour of λ^* of (4.9) for $\varepsilon \ll 1$ and $\beta \ll 1$ such that $\beta = \beta_0\varepsilon^2$, where $\beta_0 = \mathcal{O}(1)$. To do so we assume that the bifurcation curve of (4.9) (seen in Figure 6) is given by the graph $(\lambda(\alpha;\varepsilon),\alpha)$, where $\alpha := u(0)$. We also denote the fold corresponding to λ^* as $(\lambda^*(\varepsilon),\alpha^*(\varepsilon))$, where $\lambda^*(\varepsilon) = \lambda(\alpha^*(\varepsilon);\varepsilon)$, and determine it by the condition $\mathrm{d}\lambda/\mathrm{d}\alpha(\alpha^*) = 0$. With this setup, we expand u and λ as

$$u(r;\alpha,\varepsilon) = u_0(r;\alpha) + \varepsilon^2 u_1(r;\alpha) + \mathcal{O}(\varepsilon^4), \quad \lambda(\alpha;\varepsilon) = \lambda_0(\alpha) + \varepsilon^2\lambda_1(\alpha) + \mathcal{O}(\varepsilon^4),$$

https://doi.org/10.1017/S0956792512000435 Published online by Cambridge University Press

which after inserting into problem (4.9) implies that u_0 and u_1 satisfy

$$u_0'' + \frac{1}{r}u_0' = \frac{\lambda_0}{(1+u_0)^2}, \quad 0 < r < 1; \qquad u_0'(0) = 0,\ u_0(1) = 0, \tag{4.31}$$

$$\mathscr{L}u_1 = \frac{3\lambda_0(u_0')^2 + 2\lambda_1}{2(1+u_0)^2} - \frac{(u_0')^3}{r} + \beta_0, \quad 0 < r < 1; \qquad u_1'(0) = 0,\ u_1(1) = 0, \tag{4.32}$$

where $\mathscr{L}$ is the operator defined in (3.23).

Then to determine the asymptotic behaviour of λ^*, we expand λ^* and α^* as

$$\lambda^*(\varepsilon) = \lambda(\alpha^*;\varepsilon) = \lambda_0(\alpha^*) + \varepsilon^2\lambda_1(\alpha^*) + \mathscr{O}(\varepsilon^4), \quad \alpha^*(\varepsilon) = \alpha_0 + \varepsilon^2\alpha_1 + \mathscr{O}\left(\varepsilon^4\right).$$

Following similar steps as in Section 3.1.2 except that β is replaced by ε^2, we find that the two-term expansion for λ^* is given by

$$\lambda^*(\varepsilon) = \lambda_0(\alpha_0) + \varepsilon^2\lambda_1(\alpha_0) + \mathscr{O}\left(\varepsilon^4\right), \tag{4.33}$$

where $\lambda_0(\alpha_0)$ is λ^* for the unperturbed problem (4.31). To find $\lambda_1(\alpha_0)$, we use the Fredholm solvability condition as in Section 3.1.2. That is, since $\partial_\alpha u_0|_{\alpha=\alpha_0}$ satisfies the homogeneous version of problem (4.32), we need it to be orthogonal with respect to the L^2 inner product to the right-hand side of (4.32):

$$\int_0^1 (\partial_\alpha u_0)\left[\frac{3\lambda_0(u_0')^2 + 2\lambda_1}{2(1+u_0)^2} - \frac{(u_0')^3}{r} + \beta_0\right]\Bigg|_{\alpha=\alpha_0} r\,\mathrm{d}r = 0.$$

In solving this equation for $\lambda_1(\alpha_0)$, we find that the order $\mathscr{O}(\varepsilon^2)$ term of (4.33) is

$$\varepsilon^2\lambda_1(\alpha_0) = \beta\frac{-\int_0^1 (\partial_\alpha u_0)|_{\alpha=\alpha_0}\, r\,\mathrm{d}r}{\int_0^1 (\partial_\alpha u_0)(1+u_0)^{-2}|_{\alpha=\alpha_0}\, r\,\mathrm{d}r} + \varepsilon^2\frac{\int_0^1 (\partial_\alpha u_0)(u_0')^2\left[(u_0') - (3/2)\lambda_0 r(1+u_0)^{-2}\right]\big|_{\alpha=\alpha_0}\mathrm{d}r}{\int_0^1 (\partial_\alpha u_0)(1+u_0)^{-2}|_{\alpha=\alpha_0}\, r\,\mathrm{d}r},$$

yielding the following asymptotic result for λ^* of problem (4.9).

Principle Result 4.1 *Let (λ_0, α_0) be the fold point corresponding to λ^* of problem* (4.31). *Then in the regime $\varepsilon \ll 1$ and $\beta \ll 1$, such that $\beta = \mathscr{O}(\varepsilon^2)$, the two-term expansion of λ^* for boundary value problem* (4.9) *is given by*

$$\lambda^*(\varepsilon, \beta) = \lambda_0 + \beta\lambda_g + \varepsilon^2\lambda_s + \mathscr{O}(\varepsilon^4), \tag{4.34}$$

where

$$\lambda_g = \frac{-\int_0^1 \varphi\, r\,\mathrm{d}r}{\int_0^1 \varphi(1+u_0)^{-2}\, r\,\mathrm{d}r}, \quad \lambda_s := \frac{\int_0^1 \varphi\,(u_0')^2\left[(u_0') - \frac{3}{2}\lambda_0(1+u_0)^{-2}\, r\right]\mathrm{d}r}{\int_0^1 \varphi(1+u_0)^{-2}\, r\,\mathrm{d}r}. \tag{4.35 a, b}$$

https://doi.org/10.1017/S0956792512000435 Published online by Cambridge University Press

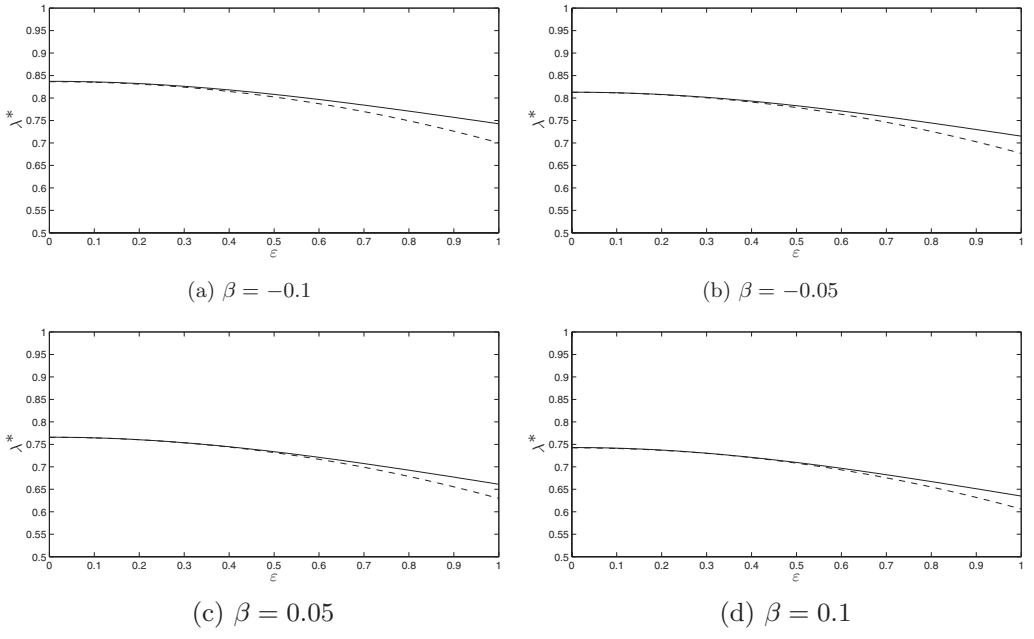

FIGURE 8. The two-term asymptotic approximation of λ^* for boundary value problem (4.9) given in (4.34) (dashed) versus the full numerical approximation (line) for various β.

Here, u_0 satisfies (4.31) *with $u_0(0) = \alpha_0$ and φ satisfies*

$$\varphi'' + \frac{1}{r}\varphi' + \frac{2\lambda_0}{(1+u_0)^3}\varphi = 0, \quad 0 < r < 1; \qquad \varphi'(0) = 0,\ \varphi(1) = 0,$$

such that $\|\varphi\|_\infty = 1$. Note that λ_g and λ_s, respectively, are the same as those defined in equations (3.25) *and* (1.4). *Recall that the subscripts g and s are used to indicate which correction is due to gravitational effects and which is due to surface effects, respectively.*

Recall that in Section 3.1.2 we have already calculated λ_g. Therefore, we calculate λ_s using (4.35 *b*) and find that the approximate expansion of λ^* for boundary value problem (4.9) is

$$\lambda^*(\varepsilon) \sim 0.7892 - 0.4709\beta - 0.1360\varepsilon^2. \tag{4.36}$$

Figure 8 provides a comparison of the computed two-term asymptotic approximation, equation (4.34), versus the full numerical approximation of λ^*. We can see that the two-term asymptotic approximation provides a very good approximation to λ^*.

5 Experimental results and comparison

In this section, we experimentally compute V^* for gravity up and down and then compare these results to the theory derived in Sections 3 and 4.

https://doi.org/10.1017/S0956792512000435 Published online by Cambridge University Press

Table 1. *Experimental data for gravity down*

	V^* (V)				
h (mm)	Trial 1	Trial 2	Trial 3	Trial 4	Average (V_d^*)
20.00	5.538e03	5.549e03	5.460e03	5.535e03	5.5205e03
23.95	7.076e03	7.162e03	7.115e03	7.169e03	7.1305e03
28.13	9.103e03	9.038e03	9.068e03	9.116e03	9.08125e03
30.83	10.183e03	10.223e03	10.227e03	10.253e03	10.2215e03
34.93	11.791e03	11.870e03	11.910e03	11.859e03	11.8575e03
38.51	13.141e03	13.153e03	13.137e03	13.171e03	13.1505e03
42.90	14.667e03	14.899e03	14.897e03	14.936e03	14.84975e03
45.83	16.228e03	16.227e03	16.264e03	16.208e03	16.23175e03

5.1 Experimental setup and results

Our experimental setup follows that of Section 3 in [22]. Specifically it consists of two $15.5 \times 15.5 \times 3$ mm acrylic plates that are coated with conductive aluminium and separated by a distance h. In the case where gravity is pointing down (up) in the z-direction, the upper (lower) plate has a hole cut in its centre while the lower (upper) plate remains solid. The two plates are connected in each corner by insulating nylon 6/6 threaded rods. To change the separation, stacks of 0.7 mm thick nylon 6/6 flat washers are added. Then a soap film – consisting of 800 mL of distilled water, 50 mL of glycerin and 135 mL of original Dawn soap – is applied across the hole of the upper (lower) plate. The upper plate is linked to a Glassman High Voltage power supply (model: PS/WR 100P2.5DM1) and set to a voltage V, while the bottom plate is grounded. Thus, a potential difference is created between the plates, creating an electric field that causes the soap film to deflect towards the bottom (top) plate.

Starting with a small plate separation, we increase the voltage until the soap film collapses or 'pulls-into' the solid plate. The voltage at which this occurs is the pull-in voltage, V^*, and is recorded along with the corresponding plate separation h. This is done four times. Then, the separation is increased and the experiment is repeated. This process continues until h becomes too large for accurate measurements. These recorded measurements (h, V^*) determine the data set for which we can compare our previous theoretical work.

The surface tension, γ, is measured with a SITA Dyno Tester tensiometre to be 25.4 dyn/cm. Therefore, each parameter needed for experimental and theoretical comparison is known. The experimental data are given in Tables 1 and 2 with a comparison shown in Figure 9. From this, it is seen that experimentally the difference between gravity up and down is small.

5.2 Comparison with theory

Recall that the two-term asymptotic approximation of λ^* for models (3.4) and (4.9) are given by

$$\lambda^*(\beta) = \lambda_0 + \beta\lambda_g + \mathcal{O}(\beta^2) \tag{3.25}$$

https://doi.org/10.1017/S0956792512000435 Published online by Cambridge University Press

Table 2. *Experimental data for gravity up*

	V^* (V)				
h (mm)	Trial 1	Trial 2	Trial 3	Trial 4	Average (V_{d}^*)
20.00	5.851e03	5.888e03	5.962e03	5.851e03	5.8880e03
23.95	7.277e03	7.526e03	7.537e03	7.300e03	7.4100e03
28.13	9.345e03	9.349e03	9.383e03	9.445e03	9.3805e03
30.83	10.483e03	10.530e03	10.509e03	10.543e03	10.5162e03
34.93	12.207e03	12.244e03	12.221e03	12.187e03	12.2147e03
38.51	13.393e03	13.437e03	13.403e03	13.447e03	13.4200e03
42.90	15.489e03	15.554e03	15.564e03	15.537e03	15.5360e03
45.83	16.596e03	16.699e03	16.741e03	16.730e03	16.6915e03

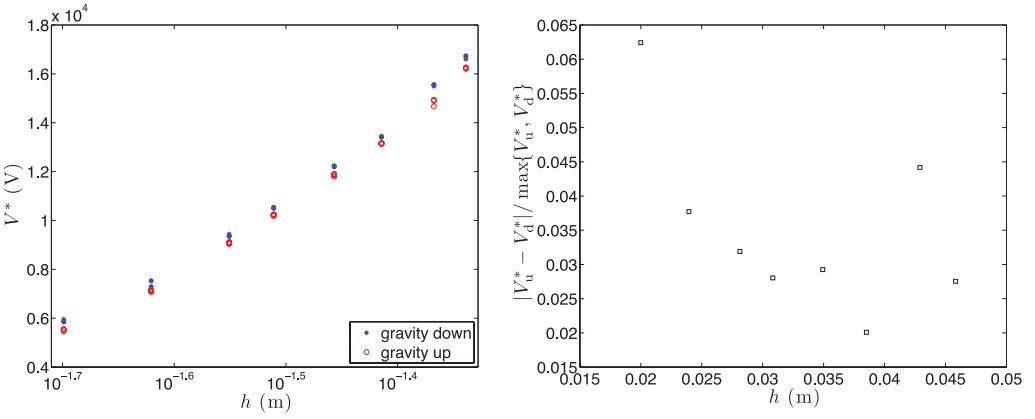

FIGURE 9. (Colour online) (a) Experimental data for the pull-in voltage V^* for gravity down (asterisk) and gravity up (circle). (b) The plate separation h versus the measure of the difference between the data for gravity down and up, $|V_{\mathrm{u}}^* - V_{\mathrm{d}}^*|/\max\{V_{\mathrm{u}}^*, V_{\mathrm{d}}^*\}$, for each fixed h.

and

$$\lambda^*(\varepsilon, \beta) = \lambda_0 + \beta\lambda_g + \varepsilon^2\lambda_s + \mathcal{O}(\varepsilon^4), \tag{4.34}$$

respectively. Therefore, using the definitions of β and ε, we deduce that

$$V^* = \frac{\rho g \ell L \lambda_g}{\sqrt{2\varepsilon_0\gamma\lambda_0}} h^{1/2} + \frac{\sqrt{2\gamma\lambda_0}}{\sqrt{\varepsilon_0}L} h^{3/2} + o(h^{3/2}) \tag{5.1}$$

and

$$\begin{aligned} V^* = {} & \frac{\rho g \ell L \lambda_g}{\sqrt{2\varepsilon_0\gamma\lambda_0}} h^{1/2} + \frac{\sqrt{2\gamma\lambda_0}}{\sqrt{\varepsilon_0}L} h^{3/2} \\ & - \frac{\rho g \ell \lambda_s \lambda_g}{2\sqrt{2\varepsilon_0\gamma\lambda_0{}^3}L} h^{5/2} + \frac{\lambda_s\sqrt{\gamma}}{\sqrt{2\varepsilon_0\lambda_0}L^3} h^{7/2} + o(h^{7/2}) \end{aligned} \tag{5.2}$$

are the predicted pull-in voltages of (3.4) and (4.9), respectively. A comparison of prediction (5.1) and (5.2) are shown in Figure 10 along with the experimental data. Comparing

https://doi.org/10.1017/S0956792512000435 Published online by Cambridge University Press

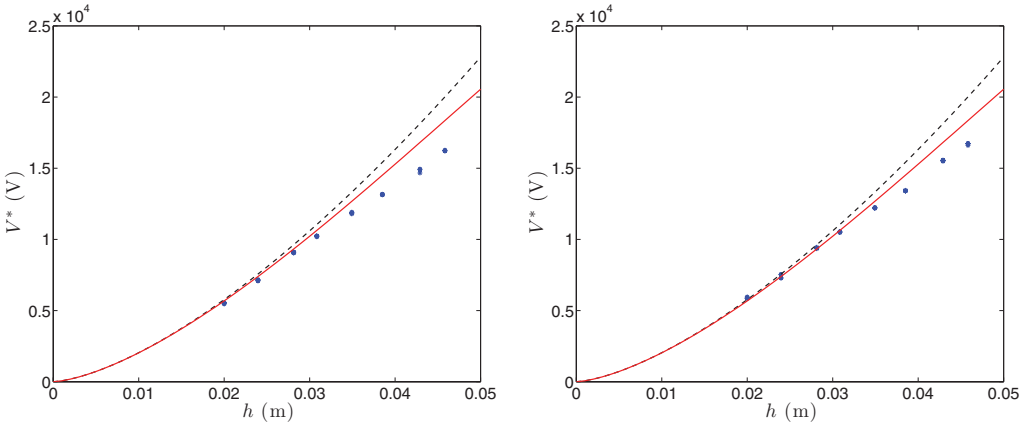

(a) Gravity down (b) Gravity up

FIGURE 10. (Colour online) Predicted pull-in voltages, V^*, of (5.1) (dashed line) and (5.2) (line) versus the plate separation h with the experimental data (asterisk) from Section 5.1.

with Figure 2 we see that (5.1) and (5.2) provide little correction for larger h; in particular, the terms in (5.2) arising effect of gravity are multiple orders of magnitude smaller than the other terms.

6 Conclusion

In this paper, our goal was to investigate the effect of gravity on the generalized version of G. I. Taylor's experiment (Figure 1). From this we hoped to resolve the discrepancy, seen in Figure 2, between the predicted and the experimental values of the pull-in voltage V^* for electrostatically actuated soap films (cf. [4,22]).

To achieve our goal we first formed a generalized model that included surface, electrostatic and gravitational effects. From commonly used assumptions we then reduced this general model into two nonlinear eigenvalue problems: (3.1) and (4.1). Using a mix of rigor and formal asymptotics, we investigated the behaviour of their solutions sets. Most importantly, we showed that no solutions of these models exist when the nonlinear eigenvalue λ gets too large (Theorems 3.1 and 4.5). Since λ is proportional to the applied voltage squared, this behaviour implies that a pull-in voltage V^* exists. Next for both models we constructed a two-term asymptotic approximation that explicitly described the behaviour of V^* and compared it to experimental data gathered in Section 5. From this comparison, we showed (both experimentally and theoretically) that gravity has minimal effect on the system in question and cannot be the cause of the discrepancy. Therefore, from the modelling done in Section 2, it seems that the difference is most likely due the approximation made in the electric field – specifically the dropping of the fringing fields.

Acknowledgements

The first author (N.D.B.) thanks the National Science Foundation for their support through a Graduate Research Fellowship. The last author (J.A.P.) thanks the National Science Foundation (NSF) Award No. 312154.

References

[1] Ackerberg, R. C. (1969) On a nonlinear differential equation of electrohydrodynamics. *Proc. R. Soc. Lond. Ser. A Math. Phys. Eng. Sci.* **312**, 129–140.

[2] Beckham, J. R. (2008) *Analysis of Mathematical Models of Electrostatically Deformed Elastic Bodies*, dissertation, University of Delaware.

[3] Brubaker, N. D. & Lindsay, A. E. (Preprint) The onset of multivalued solutions of a prescribed mean curvature equation with singular nonlinearity.

[4] Brubaker, N. D. & Pelesko, J. A. (2011) Non-linear effects on canonical MEMS models. *Eur. J. Appl. Math.* **22**, 455–470.

[5] Brubaker, N. D. & Pelesko, J. A. (2012) Analysis of a one-dimensional prescribed mean curvature equation with singular nonlinearity. *Nonlinear Anal.* **75**, 5086–5102.

[6] Coddington, E. A. & Levinson, N. (1955) *Theory of Ordinary Differential Equations*, International Series in Pure and Applied Mathematics, McGraw-Hill, New York.

[7] Finn, R. (1986) *Equilibrium Capillary Surfaces*, no. 284 in Grundlehren der mathematischen Wissenschaften, Springer-Verlag, New York.

[8] Gidas, B., Ni, W.-M. & Nirenberg, L. (1979) Symmetry and related properties via the maximum principle. *Comm. Math. Phys.* **68**, 209–243.

[9] Gilbarg, D. & Trudinger, N. S. (1983) *Elliptic Partial Differential Equations of Second Order*, no. 224 in Grundlehren der mathematischen Wissenschaften, 2nd ed., Springer-Verlag, Berlin.

[10] Guo, Y., Pan, Z. & Ward, M. J. (2005) Touchdown and pull-in voltage behavior of a MEMS device with varying dielectric properties. *SIAM J. Appl. Math.* **66**, 309–338.

[11] Jackson, J. D. (1999) *Classical Electrodynamics*, 3rd ed., Wiley, New York.

[12] Lindsay, A. E. & Ward, M. J. (2008) Asymptotics of some nonlinear eigenvalue problems for a MEMS capacitor. Part I: Fold point asymptotics. *Methods Appl. Anal.* **15**, 297–326.

[13] Lindsay, A. E. & Ward, M. J. (2011) Asymptotics of some nonlinear eigenvalue problems modelling a MEMS capacitor. Part II: Multiple solutions and singular asymptotics. *Eur. J. Appl. Math.* **22**, 83–123.

[14] Mellet, A. & Vovelle, J. (2010) Existence and regularity of extremal solutions for a mean-curvature equation. *J. Differ. Equ.* **249**, 37–75.

[15] Moulton, D. E. & Pelesko, J. A. (2008) Theory and experiment for soap-film bridge in an electric field. *J. Colloid Interface Sci.* **322**, 252–262.

[16] Pan, H. (2009) One-dimensional prescribed mean curvature equation with exponential nonlinearity. *Nonlinear Anal.* **70**, 999–1010.

[17] Pelesko, J. A. (2001) Electrostatic field approximations and implications for MEMS devices. In: *ESA Annual Meeting Proceedings*, East Lansing, MI, pp. 126–137.

[18] Pelesko, J. A. & Bernstein, D. H. (2003) *Modeling MEMS and NEMS*, Chapman & Hall/CRC, Boca Raton, FL.

[19] Pelesko, J. A. & Chen, X. Y. (2003) Electrostatic deflections of circular elastic membranes. *J. Electrost.* **57**, 1–12.

[20] Pelesko, J. A. & Driscoll, T. A. (2005) The effect of the small-aspect-ratio approximation on canonical electrostatic MEMS models. *J. Engrg. Math.* **53**, 239–252.

[21] Protter, M. H. & Weinberger, H. F. (1967) *Maximum Principles in Differential Equations*, Springer, New York.

[22] Siddique, J. I., Deaton, R., Sabo, E. & Pelesko, J. A. (2011) An experimental investigation of the theory of electrostatic deflections. *J. Electrost.* **69**, 1–6.

[23] Taylor, G. I. (1968) The coalescence of closely spaced drops when they are at different electric potentials. *Proc. R. Soc. Lond. Ser. A Math. Phys. Eng. Sci.* **306**, 423–434.

[24] Van de Velde, E. V. & Ward, M. J. (1991) Criticality in reactors under domain or external temperature perturbations. *Proc. Roy. Soc. London Ser. A* **434**, 341–367.